International Journal of Thermophysics, Vol. 28, No. 1, February 2007 (© 2006)
DOI: 10.1007/s10765-006-0135-1

Thermal and Electrical Properties of a Suspended Nanoscale Thin Film

X. Zhang,[1,2] H. Q. Xie,[1] M. Fujii,[1] H. Ago,[1] K. Takahashi,[3] T. Ikuta,[3] H. Abe,[4] and T. Shimizu[4]

Received July 5, 2005

This paper reports on measurements of in-plane thermal conductivities, electrical conductivities, and Lorentz number of two microfabricated, suspended, nanosized thin films with a thickness of 28 nm. The effect of the film thickness on the in-plane thermal conductivity is examined by measuring other nanofilm samples with a thickness of 40 nm. The experimental results show that the electrical conductivity, resistance–temperature coefficient, and in-plane thermal conductivity of the nanofilms are much smaller than the corresponding bulk values from 77 to 330 K. However, the Lorentz number of the nanofilms is about two times that of the bulk value at room temperature, and even up to three times that of the bulk value at 77 K. These results indicate that the relation between the thermal conductivity and electrical conductivity of the nanofilms does not follow the Wiedemann–Franz law for bulk metallic materials.

KEY WORDS: electrical conductivity; Lorentz number; nanofilm; thermal conductivity.

1. INTRODUCTION

The thermal and electrical properties of thin films play vital roles in determining the performance of many components and devices used in modern engineering systems. Many measurements have demonstrated that

[1] Institute for Materials Chemistry and Engineering, Kyushu University, Kasuga 816–8580, Japan.
[2] To whom correspondence should be addressed. E-mail: xzhang@cm.kyushu-u.ac.jp
[3] Graduate School of Engineering, Kyushu University, Fukuoka 812–8581, Japan.
[4] Nanotechnology Research Institute, National Institute of Advanced Industrial Science and Technology, Tsukuba 305–8562, Japan.

0195-928X/07/0200-0033/0 © 2006 Springer Science+Business Media, LLC

the thermal conductivities of various thin films, as well as the electrical conductivities of electrically conductive thin films, are much smaller than those of their corresponding bulk materials [1–6]. The difference in the conductivities between thin films and bulk materials is considered to be caused by the structure defect [7], boundary scattering (surface scattering [8–10], and grain boundary scattering [11–13]).

For metallic thin films, theoretical models based on carrier scattering have been proposed to predict the conductivities. In most of the considerations, the thermal conductivity of a thin film is calculated from its proportional relation to the electrical conductivity via the Wiedemann–Franz law [14–16] or a similar analogy [9]. Several experimental studies investigated either the thermal conductivity or the electrical conductivity and used the electrical–thermal relation to determine the other property [17, 18]. Although two methods [19, 20] that were used to measure the thermal conductivity and specific heat may also be used to measure the electrical conductivity, very few investigations deal with both conductivities together. Furthermore, most of the previously studied thin films are deposited on substrates and the considerations of the effects caused by the substrates are not sufficient.

For this reason, we report on measurements of the in-plane thermal conductivity of suspended Pt nanofilms, for which there is no effect caused by a substrate. Also a four-wire method is used to measure the electrical resistance. Results show that the electrical conductivity, resistance–temperature coefficient, and in-plane thermal conductivity of the nanofilms are much smaller than the corresponding bulk values, but the Lorentz numbers are larger than the corresponding bulk values.

2. EXPERIMENTAL

Figure 1 shows the fabrication processes of the suspended Pt nanofilm. These processes include electron beam (EB) lithography, EB physical vapor deposition (EBPVD), and isotropic/anisotropic etching techniques. A Si (100) wafer with a SiO_2 layer of 180 nm is used as the starting material. First, a resist layer is spin-coated to be 320 nm thick. By using an electron beam lithography system, the patterns of the nanofilm and the leads are directly drawn on the resist. In the next step, a titanium film of 5 nm and a platinum film of 28 nm are deposited subsequently with the EBPVD method. The titanium film is used only for adhesion. Then a lift-off technique is applied, in which the chip is immersed in a liquid resist-remover to leave only the Pt/Ti pattern on the SiO_2 layer. An isotropic

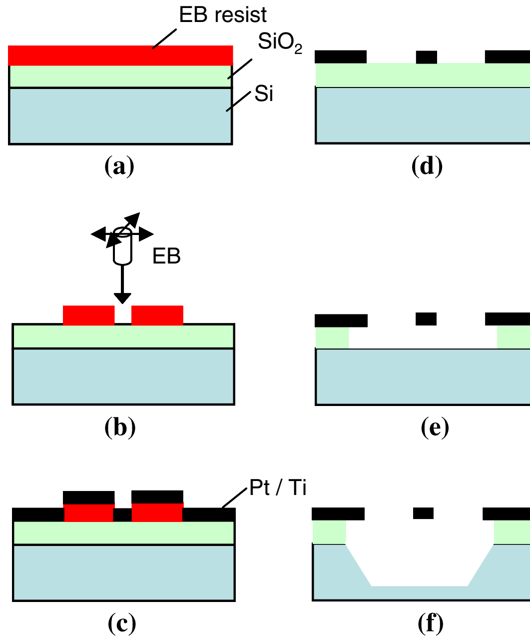

Fig. 1. Fabrication processes of nanofilm.

etching using a buffered hydrofluoric acid is applied to remove the SiO_2 layer around the Pt nanofilm. The titanium layer is also etched away in this process. The Si is partly etched out using KOH solution, leaving a gap of 6 μm between the suspended nanofilm and the substrate.

Figure 2 illustrates the scanning electron micrograph of the suspended Pt nanofilm and an electrical circuit for measuring the electrical and thermal properties. The thickness of two prepared nanofilms (image in Fig. 2a) is 28 nm, and the width and length of the nanofilms are 332 and 339 nm, and 5.37 and 5.31 μm, respectively. As shown in Fig. 2b, the measurement system consists of the nanofilm sample, two digital multimeters (Keithley 2002, 8.5 digits), a standard resistance (Yokogawa 2792), and a power supply (Advantest R6243). In all the measurements, the silicon chip with the suspended nanofilm is mounted on the sample holder of a liquid nitrogen cryostat (Oxford Instruments, Optistat DN-V), where the sample chamber is continuously evacuated by a vacuum pump and a molecular pump, and the temperature of the sample holder can be controlled continuously from 77 to 500 K.

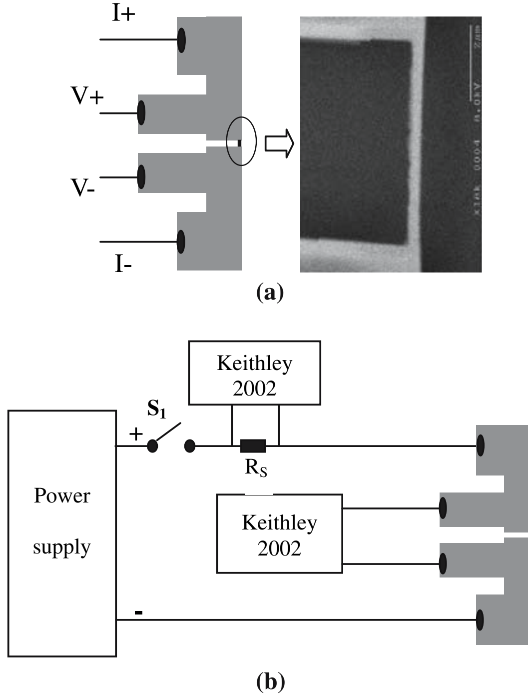

Fig. 2. (a) Scanning electron micrograph of the suspended Pt film and (b) measurement system. The top right image is the real structure of the part marked by a circle in the top left figure (a).

3. RESULTS AND DISCUSSION

Figure 3 shows the measured electrical resistance. Figure 3a shows the dependence of the electrical resistance (R) on the heating rate (q) for sample B at 190 K. There is a linear relation between the resistance and heating rate. The intrinsic electrical resistance at 190 K is the value for which $q = 0\,\mu$W, and can be obtained accurately by using a least-squares fit. These intrinsic resistances for the temperatures ranging from 77 to 320 K are plotted in Fig. 3b. Each value is the average of three measurements. The maximum dispersion is within 0.005%. As shown in Fig. 3b, the electrical resistance increases smoothly with an increase in temperature. The electrical conductivity (σ) is calculated from $\sigma = l/(wdR)$, where l, w, and d are the length, width, and thickness of the film, respectively. For comparisons with bulk values, the resistance–temperature coefficient (β) is determined from the measured resistances at different temperatures

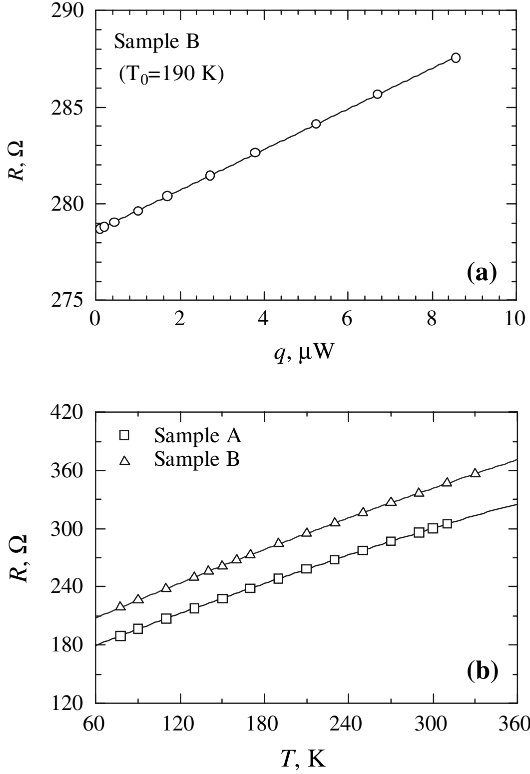

Fig. 3. (a) Dependence of the resistance on the heating rate and (b) dependence of the resistance on the temperature.

by using the expression $\beta = \Delta R/(R_0 \Delta T)$, where R_0 is the resistance at 0°C. It is seen from Fig. 4a that the electrical conductivities of the nanofilms are much smaller compared to the bulk values. For example, at 300 K, the measured electrical conductivities are about $(1.78\text{–}1.90)\times 10^6\,\Omega^{-1}\cdot\text{m}^{-1}$, less than one fifth of the bulk value of $9.50 \times 10^6\,\Omega^{-1}\cdot\text{m}^{-1}$. The weak electrically conductive capacity of the nanofilms might be ascribed to the structure defect formed during fabrication and to the boundary scattering of electrons [8]. Furthermore, the measured resistance–temperature coefficients of the nanofilms are significantly lower than the corresponding bulk values (Fig. 4b). The resistance–temperature coefficients of the nanofilms, which are about $0.0014\text{–}0.0016\,\text{K}^{-1}$ at 300 K, are less than half of that of the bulk value of $0.0039\,\text{K}^{-1}$.

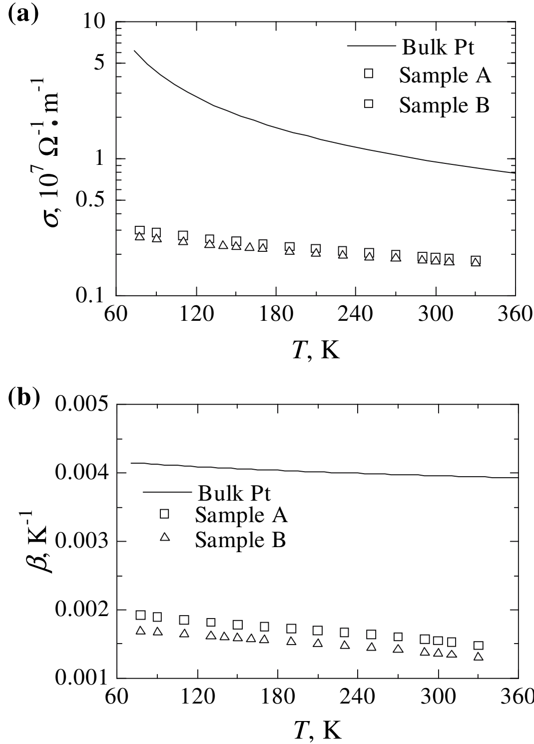

Fig. 4. (a) Dependence of the electrical conductivity on the temperature and (b) dependence of the resistance coefficient on the temperature.

The temperature-dependent in-plane thermal conductivity of the nanofilm can be measured accurately by a one-dimensional steady-state method. In the measurements, the nanofilm serves both as a heating source with a homogeneous heat flux and as an electrical thermometer. Initially, the nanofilm and the leads are kept in thermal equilibrium at a set temperature of T_0. When a constant heating direct current flows through the nanofilm, it is heated and subjected to one-dimensional heat transfer. The result of a transient heat transfer simulation has shown that the temperature distribution in this nanofilm reaches steady-state after heating for several μs, which indicates it is reasonable to assume steady-state heat transfer in the nanofilm in the measurements. All the measurements are carried out at a high vacuum level of $\sim 3 \times 10^{-6}$ Torr and at set temperatures ranging up to 320 K to suppress residual gas

conduction and radiation loss. Therefore, the heat transfer is dominated by one-dimensional steady-state heat conduction along the length direction and the temperature distribution along the nanofilm, $T(x)$, is expressed as follows:

$$T(x) = T_0 + \frac{IV}{2wd\lambda}x - \frac{IV}{2lwd\lambda}x^2 \quad (1)$$

where x is the distance from the connection of the nanofilm and the lead which serves as a heat sink where the temperature is kept at T_0 during the measurement, I is the heating current, V is the applied voltage, and λ is the thermal conductivity. The average temperature increase along the nanofilm, ΔT_L, is calculated from Eq. (1) and the thermal conductivity is determined from the following formula:

$$\lambda = \left(\frac{l}{12wd}\right) \Big/ \left(\frac{\Delta T_L}{IV}\right) \quad (2)$$

In the experiments, I and V are recorded while the applied current is increased up to a value in the range of 150–250 μA depending on the set temperature T_0. Figure 5a shows the temperature increase as a function of the heating rate. Here $q = IV$. ΔT_L is calculated from the electrical resistance increase during heating by using the expression $\Delta T = \Delta R/(\beta R_0)$. It is observed that ΔT_L increases linearly with q, and this linear relation enables us to extract $\Delta T_L/q$ by using a least-squares fit. At the same heating rate, the temperature increase is changed with a different set temperature (Fig. 5a), indicating that the thermal conductivity of the nanofilm is changed with the different set temperature. The thermal conductivity of the nanofilm is calculated using Eq. (2) and is shown in Fig. 5b. From Fig. 5b, it is observed that the thermal conductivity of the nanofilm increases with temperature. It is further obvious that the measured thermal conductivities at different temperatures are much lower than the corresponding bulk values. For example, at room temperature the bulk value of the thermal conductivity of Pt is 71.4 $W \cdot m^{-1} \cdot K^{-1}$, whereas those of the present measurements are 26.5 and 27.3 $W \cdot m^{-1} \cdot K^{-1}$, less than half of the bulk value.

The uncertainty of the thermal conductivity measurements can arise from errors in measurements of voltage, current, temperature, and dimensions of the nanofilm. In our previous paper [21], the electrical and thermal conductivities of five nanofilm samples with the same thickness of 40 nm, but different widths from 360 to 600 nm and a length of about 6.0 μm were measured at room temperature. The measured results showed that the effects of the electrical spreading resistance between the ends of

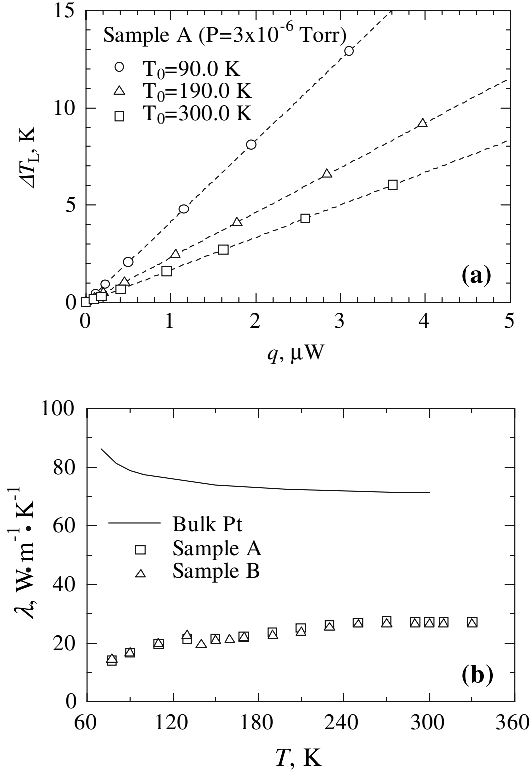

Fig. 5. (a) Temperature increase as a function of the heating rate and (b) thermal conductivity as a function of temperature.

the nanofilm and the voltage probes (V+ and V− in Fig. 2) were negligible. The width and length of the nanosensor are measured with a scanning electron microscope, and the film thickness is measured with a calibrated quartz crystal thin film thickness monitor (CRTM-7000 with a resolution of 0.01 nm). The error caused by the dimension measurements is estimated to be less than ±3%. Therefore, the overall error of the thermal conductivity is estimated to be within ±5%.

Previous studies state that since the thermal conductivity of a pure bulk sample is proportional to the electrical conductivity of the same sample via the Wiedemann–Franz law, the reduced thermal conductivity of thin films must also have the same proportionality with the reduced electrical conductivity of the same films [15–18]. It is worth noting, however, that the ratio of the thermal conductivity to the electrical conductivity,

calculated from the present measurements, is about $(1.4–1.5)\times10^{-5}$ $\mathrm{W\cdot\Omega\cdot K^{-1}}$ at 300 K, whereas that of the bulk platinum is about 7.5×10^{-6} $\mathrm{W\cdot\Omega\cdot K^{-1}}$. This remarkable difference indicates that the relation between the thermal conductivity and electrical conductivity of these nanoscale metallic thin films does not follow the Wiedemann–Franz law that determines the relation between the thermal conductivity and electrical conductivity of a bulk metallic material. The effects of material type, fabrication method, and the film sizes need to be taken into account. Therefore, considerable care should be taken when we estimate the thermal conductivity from the electrical conductivity for metallic nanofilms.

Figure 6 shows the effect of the film thickness on the thermal conductivity. The thermal conductivities of two other samples C and D with a thickness of 40 nm, lengths of 5.58 and 5.67 μm, and widths of 362 and 381 nm are measured at room temperature. As shown in this figure, the thermal conductivity increases with an increase in the film thickness. This tendency is the same as in the previous study [22].

Figure 7 further shows a comparison of the Lorentz numbers, $L=\lambda/(\sigma T_0)$, obtained for both the Pt nanofilm and bulk material. The Lorentz number in the present study can be calculated directly using $L=\beta R_o V^2/(12\Delta R T_0)$, which is independent of the dimensions of the nanofilm. For the Pt nanofilm the Lorentz number decreases with an increase in temperature; for the Pt bulk material it slightly increases with increasing temperature. The Lorentz numbers of the nanofilms are about two times that of the bulk value at room temperature, and even up to three times that of the bulk value at 77 K.

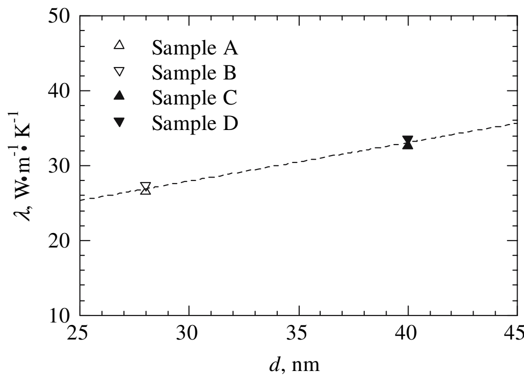

Fig. 6. Effect of the film thickness on the thermal conductivity.

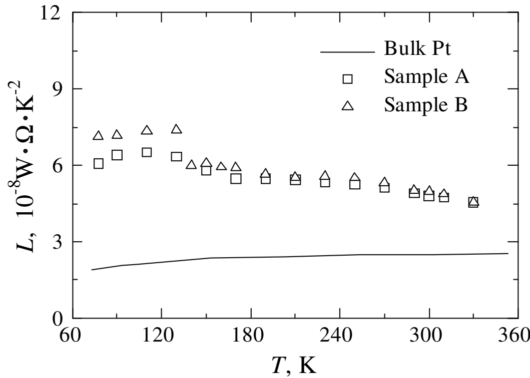

Fig. 7. Comparison of the Lorentz numbers obtained for both the Pt nanofilm and bulk material.

4. CONCLUSIONS

The thermal and electrical properties of suspended Pt nanofilms have been investigated experimentally. The measured in-plane thermal conductivity is less than half of the corresponding bulk value. This nanofilm has significantly lower electrically conductive capacity than the bulk platinum. Also, the resistance–temperature coefficients of the nanofilm are much smaller compared to the bulk data. However, the Lorentz number of the nanofilm is larger than that of the corresponding bulk material. The steady-state method presented here is applicable to the measurement of the thermal conductivity of metallic nanofilms as well as metallic nanowires that have a linear dependence of resistance with temperature over an appropriate temperature range.

ACKNOWLEDGMENTS

This work is supported partly by the Grant-in-Aid for Scientific Research B15360114 from the Ministry of Education, Science, Sports, and Culture of Japan.

REFERENCES

1. D. G. Cahill, H. E. Fischer, T. Klitsner, E. T. Swartz, and R. O. Phol, *J. Vac. Sci. Technol.* **A7**:1259 (1989).
2. X. Zhang and P. Grigoropoulos, *Rev. Sci. Instrum.* **66**:1115 (1995).
3. C. L. Tien, A. Majumdar, and F. M. Gerner, *Microscale Energy Transport* (Taylor & Francis, Washington, DC, 1998).

4. Y. S. Ju and K. E. Goodson, *Appl. Phys. Lett.* **74**:3005 (1999).
5. D. G. Cahill, W. K. Ford, K. E. Goodson, G. D. Mahan, A. Majumdar, H. J. Maris, R. Merlin, and S. R. Phillpot, *J. Appl. Phys.* **93**:793 (2003).
6. D. Song and G. Chen, *Appl. Phys. Lett.* **84**:687 (2004).
7. A. Redondo and J. G. Beery, *J. Appl. Phys.* **60**:3882 (1996).
8. K. Fuchs, *Proc. Cambridge Philos. Soc.* **34**:100 (1938).
9. S. Kumar and G. C. Vradis, *J. Heat Transfer* **116**:28 (1994).
10. G. Chen, *J. Heat Transfer* **119**:220 (1997).
11. A. F. Mayadas, M. Shatzkes, and J. F. Janak, *Appl. Phys. Lett.* **14**:345 (1969).
12. J. R. Sambles, K. C. Elsom, and D. J. Jarvis, *Philos. Trans. R. Soc. London, Ser. A* **304**:365 (1982).
13. J. W. C. de Vries, *Thin Solid Films* **167**:25 (1988).
14. C. Kittel, *Introduction to Solid State Physics, 6th Ed.* (Wiley, New York, 1986).
15. C. L. Tien, B. F. Armaly, and P. S. Jagannathan, *Thermal Conductivity* (Plenum Press, New York, 1969), p. 13.
16. C. R. Tellier and A. J. Tosser, *Size Effects of Thin Films* (Elsevier, New York, 1982).
17. P. Nath and K. L. Chopra, *Thin Solid Films* **20**:53 (1974).
18. B. Clemens, G. L. Eesley, and C. A. Paddock, *Phys. Rev. B* **37**:1085 (1988).
19. L. Lu, W. Yi, and D. L. Zhang, *Rev. Sci. Instrum.* **72**:2996 (2001).
20. Y. C. Tai, C. H. Mastrangelo, and R. S. Muller, *J. Appl. Phys.* **63**:1442 (1988).
21. X. Zhang, H. Q. Xie, M. Fujii, K. Takahashi, H. Ago, T. Shimizu, and H. Abe, *Jpn. J. Thermophys. Prop.* **19**:9 (2005).
22. T. Yamane, S. Katayama, and M. Todoki, in *Proc. 24th Japan Symp. Thermophys. Prop.* (Jpn. Soc. Thermophys. Prop., 2003), pp. 26–28.